WALANAE FAULT KINEMATIC DEDUCED FROM GEOMETRIC GEODETIC GNSS GPS MONITORING

Dina Anggreni Sarsito [1*], *Susilo* Susilo [2], *Alfend* Rudyawan [3], *Norman Arif* Muhammad[1] , *Heri* Andreas [1] and *Dhota* Pradipta[1]

[1] Geodesy Research Division, Faculty of Earth Science and Technology, Institute of Technology Bandung, Jl. Ganesha 10 Bandung 40132 – Indonesia
[2] Geospatial Information Agency, Jl. Raya Jakarta-Bogor KM.46, Cibinong 16911-Indonesia
[3] Geodynamic and Sedimentology Research Division, Faculty of Earth Science and Technology, Institute of Technology Bandung, Jl. Ganesha 10 Bandung 40132 – Indonesia

Abstract. The western Sulawesi region has the main structural boundary, the Palu Koro Fault which divides from Palu Bay at the northest part to Central Sulawesi and continues into the Bone Gulf in southest part. In the southern part of this region, namely the South Sulawesi Arm zone, there is a Walanae fault which is defined as a sinistral wrench with a NW-SE direction that divides the South Arm of Sulawesi. This fault in the northern part is expected to continue to the northwest intersecting the Makassar Strait and unite with Paternoster-Lupar (Kalimantan) sutures and at the southest ending in Flores thrust fault. Walanae fault system did not only have one strand but was divided into 4 parts, namely the northern East Walanae Fault with a slip rate of 6.634 mm/year and the southern part with a 7.097 mm/year of slip rate, as well as the northern part of West Walanae Fault with a slip rate of 4.528 mm/year and the southern part with a slip rate of 3.270 mm/year. The northern part of Walanae fault system has opening or spreading pattern occurs that is in harmony with the formation of Walanae depression. By using simple geometric modeling, we found the fault system have 2 strain partitions with dominant sinistral strike slip pattern at southern part and combination between left lateral strike slip with thrust fault pattern at northern part.

1 Introduction

The region of Eastern Indonesia is known to be an active tectonic region with high seismic activity which often has a negative impact in the form of material losses up to the loss of life after earthquakes hit the area. Sulawesi Island, which is located in this location, is in the western boundary between Eastern Indonesia and Sunda Blok which is relatively stable compare to the eastern area. This island is a result of triple junction convergence phenomena between Eurasian Continental-Sunda Block, Indo-Australian Plate and Pacific Ocean Plate, that creates several major faults across the island. Collision between Australian Craton Eastern Arc and Sunda Block Western Arc are dominated in Sulawesi and the region also divided into four different Mesozoic-Cenozoic stratigraphic provinces namely West-Southwest Sulawesi, East Sulawesi-Northon, North Sulawesi and Banggai Sula block [1, 2, 3, 4, 5, 6, 7, 8, 9, 10] . The Sulawesi western region has a main structural boundary, the Palu Koro Fault which divides from Palu Bay at the northest part to Central Sulawesi and continues into the Bone Gulf in the southest part. In the southern part of this region, namely the South Sulawesi Arm zone, there is a fault which is defined as a central wrench with a Northwest-Southeast direction that divides the South Arm of Sulawesi. This fault in the northern part is expected to continue to the northwest intersecting the Makassar Strait and unite with Paternoster-Lupar (Kalimantan) sutures and at the southest ending in Flores thrust fault.

The fault system kinematics have been studied geologically by [11, 12, 13, 14] but has never been done in the details of the geodetic method. This fault system consists of two parallel faults with Walanae depression separated it, namely the East Walane Fault and the West Walanae Fault. [14] mentioned that both faults formed at the end of the Middle Miocene with Bone Mountains as an eastern boundary and Western Divide Mountain as western boundary. [13] conclude that a sinistral strike slip motion of East Walanae Fault has played a major role in motion and geological structural developments nowadays. All of the above explanations are represented by Figure 1. Geodetic prior research using GNSS-GPS data from 1994 - 2009 by [15] estimated one slip-rate for the entire fault system by used 2 monitoring stations, namely is [east: 4.3 ± 0.6 mm / year, north: 2.0 ± 0.4 mm / year] with a sinistral / left lateral pattern and slip deficit of [east: 0.7 ± 0.3 mm / year, north: 0.2 ± 0.1 mm / year]. Thus, the Walanae fault system can be active with a total velocity of 5.1 ± 0.6 mm / year. To learn more details about the Walanae fault kinematics, the long observation data with GNSS-GPS with robust distribution stations are used in this paper. The validation of the geodetic results are from geological studies that have been carried out by previous researchers.

* Corresponding author: dsarsito@gd.itb.ac.id

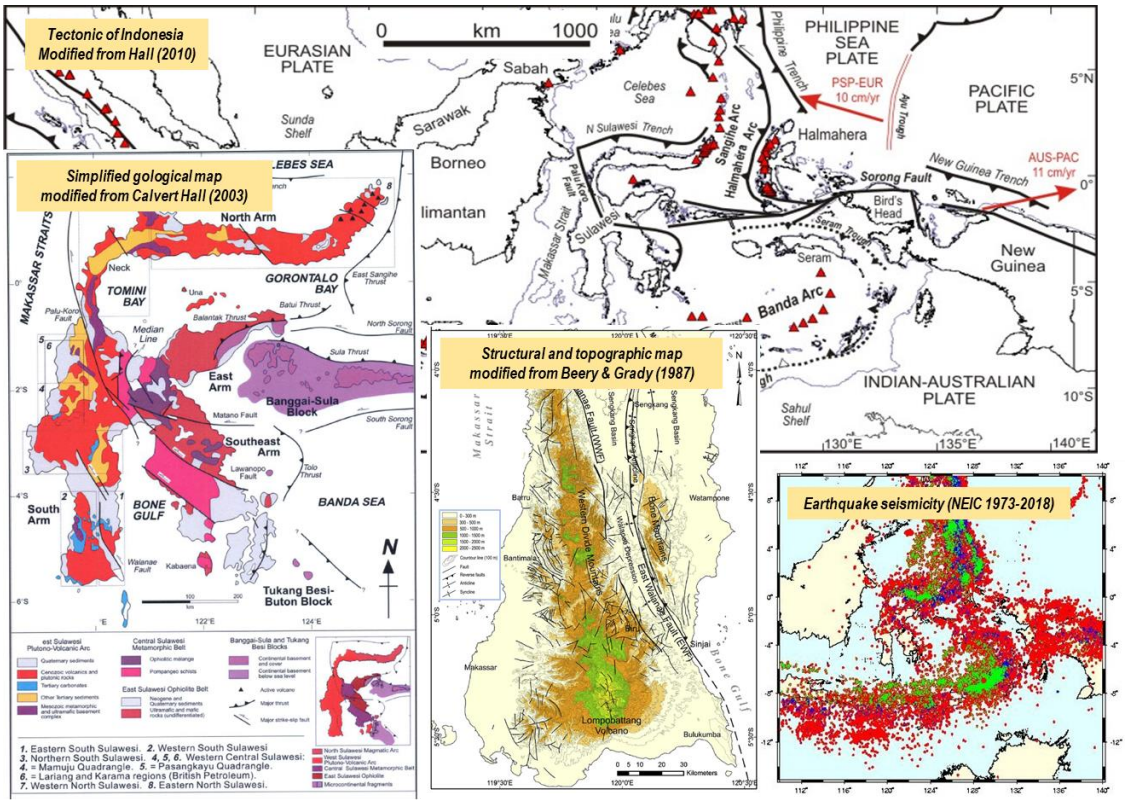

Fig 1. Tectonic of Indonesia modified from [8], Simplified feological map modified from [16], Structural and topographic map modified from [17] and Earthquake Seismicity from NEIC Catalogue (1973-2018)

2 Data and Method

GNSS-GPS Observation

The observation of GNSS-GPS in the South Arm of Sulawesi region was carried out using two methods, the first method is campaign or episodic type that carried out by the collaboration between Bakosurtanal (former) / BIG, ITB, DEOS-TU Delft and Paris ENS since GEODYSSEA Research Collaborations in 1994. This campaign type are done even though not routinely once per year for all stations in the area (UJPD, C018, C025, C026, C036 and C042). Another method we used in here is a continuous method that is managed by BIG using a fixed station measurement (CMAK and CPRE). Initially this deformation monitoring network design was dedicated to get a better understanding the kinematic pattern of the South Sulawesi Arm motion related to the need for deformation studies and the implementation of geodetic control network for mapping purposes. Furthermore, by using both episodic and continuous stations in the South Arm with a more complete and dispersed station distribution than the GNSS distribution from [15], it is expected that the Walanae fault pattern can be detected in more detail.

Data processing in this study uses GAMIT / GLOBK 10.6 GNSS processing using a multi-baseline tight constraint strategy for reference stations located outside the Eastern Indonesia zone and located in a relatively stable zone. The ITRF-2008 global terrestrial framework was mapped to obtain georeference and to obtain a local domination deformation pattern, a mapping was conducted by referring to the relatively stable Sunda Block Euler pole compared to the study area. The distribution of the observation station was originally designed to determine the rigid deformation pattern of the South Sulawesi Arm (euler pole position and rotational speed), then used for geometric initial detection of the Walanae fault movement which divides the South Arm with Northwest-Southeast direction. Since in this study two types of data were used, namely episodic and continuous, the strategy carried out would experience a slight difference in handling data for estimating survey solutions (campaign solution for episodic types), weekly solutions (weekly solution for continuous types) and time series analysis stages (time-series analysis) for estimating velocity values by correcting seismic effects of special earthquakes only for the type of continuous station using the equation of [18] as follows

$$y(t_i) = a + bt_i + c\sin(2\pi t_i) + d\cos(2\pi t_i) + e\sin(4\pi t_i) + f\cos(4\pi t_i) + \sum_{j=1}^{n_g} g_j H(t_i - T_{gj}) \sum_{j=1}^{n_h} h_j H(t_i - T_{hj})\, t_i + \sum_{j=1}^{n_k} k_j exp\left(-(t_i - T_{kj})/\tau_j\right) H(t_i - T_{kj}) + v_i \quad (1)$$

where t_i for i = 1 ... N is the epoch of the daily solution, H is the heaviside step function, coefficients a and b are the position and velocity rate of the station, coefficients c and d are annual periodic motions, coefficients e and f are semi-periodic annual motion, n_g is the number of offsets with magnitude g in the epoch T_g. Motion due to an earthquake is modeled as an exponential h and / or exponential decay with magnitude k in the epoch of earthquake T. The observation error v is assumed to be independent (not affect), identically distributed and random with error E (v) = 0. Furthermore, geometric deformation parameters are estimated using the results of the estimated diplacement vector or velocity vector of the above motion.

Geometric Deformation

To study the deformation pattern of a tectonic region, several models can be applied in order to quantify and analyze the displacement or deformation phenomena of the earth that are monitored using the GNSS-GPS geodetic method. The method of analysis in this study is a geometric method based only on observational geometric data through a simple representation of changes in the coordinates of the observation station with respect to a reference frame and homogeneous- isotropic strain parameters within a specified zone. The realization is through interpolation-extrapolation between stations without involving crustal physical parameters. From the difference between epochs for each station, we can obtain the displacement vector *d* (equation 2) or velocity rate *v* (equation 3).

$$d(n,e,u) = (n,e,u)_{tj} - (n,e,u)_{to} \quad (2)$$

$$v(n,e,u) = \frac{(n,e,u)_{tj} - (n,e,u)_{to}}{tj - to} \quad (3)$$

Where *(n, e, u)* are north, east and up displacement or velocity component, and t_o and t_j are the initial epoch and later epoch. From equation (2) or (3) it can derive translation *T*, rotation of *R* and dilation of *D* (equation (4)) deformation parameters.

$$v(n,e,u) = T + R + D \quad (4)$$

From equation (4), another deformation parameter can be described, namely Magnitude Translation T_M (equation (5)) which shows the translation magnitude in the horizontal direction and strain tensor (equation (6)) which shows the dilatation of ε_{mean} (equation (7)), pure strain ε_{pure} (equation (8)) and simple strain ε_{simple} (equation (9)) as follows

$$T_M = \left(\left(v(n)\right)^2 + \left(v(e)\right)^2 \right)^{0.5} \quad (5)$$

$$Strain\ Tensor = \begin{vmatrix} \frac{\partial v_n}{\partial n} & \frac{\partial v_e}{\partial n} \\ \frac{\partial v_n}{\partial e} & \frac{\partial v_e}{\partial ne} \end{vmatrix} = \begin{vmatrix} \varepsilon_{nn} & \varepsilon_{ne} \\ \varepsilon_{en} & \varepsilon_{ee} \end{vmatrix} \quad (6)$$

$$\varepsilon_{mean} = \frac{1}{2}(\varepsilon_{nn} + \varepsilon_{ee}) \quad (7)$$

$$\varepsilon_{pure} = \frac{1}{2}(\varepsilon_{nn} - \varepsilon_{ee}) \quad (8)$$

$$\varepsilon_{simple} = \frac{1}{2}(\varepsilon_{ne} + \varepsilon_{en}) \quad (9)$$

The above equations are then used for the geometric deformation analysis for the Walanae Fault System. The velocity rate used as the basis for the calculation is estimated in global terrestrial reference ITRF2008 to find out the consistency of the monitoring network. And to find out the deformation pattern more clearly, the velocity rate is estimated relatively to the recent Sunda Block Euler poles (51.991^0, -96.495^0, 0.291^0/My).

3 Result and Discussion

The velocity rate estimation results are divided into two part, for continuous CMAK and CPRE stations that have high reliability for the degree of solution accuracy in the ITRF2008 mapping for horizontal components namely postrms 0.003 m and 0.007 m for campaign type stations (UJPD, C018, C025 , C026, C036, C042). Figure (2 left) shows the magnitude of the velocity rate vector in the ITRF2008. From the distribution of observation stations, it can be seen that CMAK, UJPD and CPRE located in the western part of West Walanae Fault, have almost the same rate pattern (25.800 ± 0.24; -6.660 ± 0.18) mm / year, (24.720 ± 1.07; -7.630 ± 0.54) mm / year and (24.020 ± 0.17; -7.090 ± 0.29) mm / year where this indicates that the three stations are in the same region. In the Walanae Depression zone, there are three stations that also have almost the same rate stretching from north to south, namely C042, C036 and C025 with velocity rates(28.540 ± 2.06; -5.920 ± 1.60) mm / year, (28.040 ± 1.60; -5.090 ± 1.12) mm / year and (28.240 ± 1.87; -4.460 ± 1.35) mm / year. The rate of all station shows a tendency to be in the same region even though there is a slight velocity rate decreasing on the northern component of station C042 which is located northern part of C025 station in southernmost. For stations located in eastern part of the East Walanae Fault, they are C026 and C018 with velocity rate (34.890 ± 2.63; -4.190 ± 1.79) mm / year and (31.370 ± 1.87; -2.500 ± 1.35) mm / year indicating a faster velocity rate pattern compared to the stations located in Walanae Depression and in western part of West Walanae Fault. In general, it can be seen that for east-west velocity rate component, there is an increase in rate of the stations located in the western part of the South Arm to the station located on the left side of the South Arm. As for the north-south velocity components, there is generally a slowdown in the rate of motion for stations located in the northern part of the South Arm to the stations located in the southern part. A more detailed representation of the deformation pattern, the global regional effect is then eliminated by estimating the velocity rate with respect to the Sunda Block Euler Pole (Figure 2 right). Stations located in the western part of the South Arm, namely CMAK, UJPD and CPRE have

velocity rate (1.815 ± 0.24; 5.037 ± 0.18) mm / year, (0.708 ± 1.07; 4.107 ± 0.54) mm / year and (-0.332 ± 0.17 ; 4.676 ± 0.29) mm / year shows a slight decrease in absolute rate from 5.354 mm / year in the southern part to 4.678 mm / year in the northern part. For stations located in Walanae Depression, namely C042, C036 and C025, they have velocity rate of (4.111 ± 2.06; 5.907 ± 1.60) mm / year, (3.671 ± 1.60; 6.792 ± 1.12) mm / year and (4.077 ± 1.87; 7.397 ± 1.35) mm / year, which shows the pattern of absolute velocity rate decrease from southern part to the northern part, with rate 8.446 mm / year to 7.197 mm / year. For C026 and C018 stations located at eastern part of East Walanae Fault, the velocity rate are (10.701 ± 2.63; 7.766 ± 1.79) mm / year and (7.375 ± 1.87; 9.425 ± 1.35) mm / year, that shows increasing rate pattern compare to the stations which are located in Walanae Depression and in western part of West Walanae Fault. This increasing rate show different pattern compare to the previous, from southern part to the northern part, we can see the absolute increasing rate are 11.967 mm / year to 13.222 mm / year.

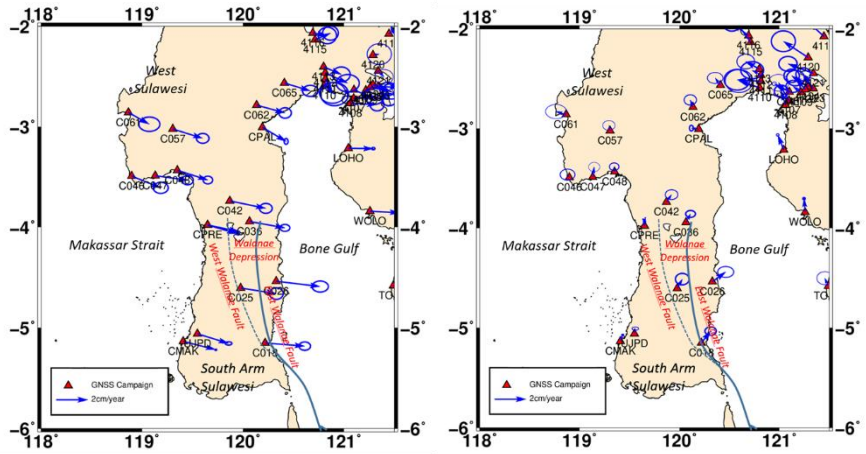

Fig. 2. Horizontal velocity rate of South Sulawesi Arm with respect to ITRF2008 (left) and Sunda Block – ITRF2008 (right)

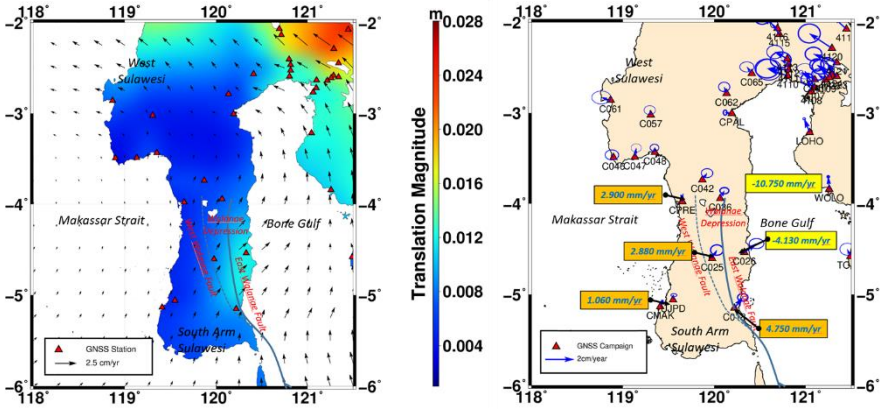

Fig. 3. Translation magnitude of horizontal velocity rate (left) and vertical velocity rate (right)

To get a clearer picture of the deformation pattern in the South Arm of Sulawesi, the horizontal velocity is described as translation magnitude (Figure 3 Left). The translation magnitude in this region ranges from 0.004 m to 0.016 m with the general pattern for the West Walane Fault region up to Walanae Depression have decreasing rate from the southern part which ranges from 0.008 m in the Makassar area to northern part up to 0.004 at the west-end of West Walanae Fault with a counter-clockwise rotation pattern for the entire South Arm. The dominance of rigid block rotation from the region above is very visible, and the velocity constraint in the northern part are estimated to be due to a collision with the Plutonic Arc Mountains in Central Sulawesi. For the eastern region of East Walanae Fault, namely Bone Mountain to the transition zone to the west at the Walanae Depression, the translation magnitude have increasing pattern from 0.008 m around Sinjai to 0.012 m in the East Sengkang Basin with counter clockwise rotation direction. The magnitude translation has gradually decrease northward to around 0.004 m in the Plutonic Arc Mountain region in Central Sulawesi. Translation magnitude generally increases from the western part of the West Walanae Fault to the eastern part of the East Walanae Fault, with a slight eastward turn in the Watampone area and looks back to the west approaching the Plutonic Arc Mountain region in the Sengkang anticline region. This indicates a long widening of the baseline dividing the east-west across Walanae Depression or showing the opening pattern. The vertical velocity rate from South Sulawesi Arm is shown in figure

3 right, where for the western part of West Walanae Fault increase vertical rate from 1.060 mm / year in the Makassar area to 2.900 mm / year in the Pare-pare area that located in the northern part. Whereas for the Walanae Depression and Bone Mountain areas located in the eastern part of the East Walanae Fault, have decreasing rate from the southern region around Sinjai with a vertical rate of 4.750 mm / year to the north, namely in the Walanae Depression area at 2.880 mm / year and East Sengkang Basin around -10,750 mm / year. This shows a difference in the increasing and decreasing patterns vertical velocity with the West Walanae Fault as a barrier, and the pattern of decline increasingly enlarges eastwards through East Walanae Fault.

Understanding the geometric pattern of deformation of the South Arm of Sulawesi is further described in Figure 4 which shows a pattern of dilation, simple shear and pure shear from the research zone. The pattern of dilatation in Figure 4 (left) shows a change of pattern that is very clearly trending north-south, namely from the region with very small dilatation approaching -0.2μs to 0.0 μs in the Plutonic Arc Mounting in the northern part, and ranging from 0.0 μs to 0.2 μs in the central region of the Sulawesi Arm which was passed by the Western Divide Mountain-Walanae Depression-Bone Mountain-East Sengkang Basin, each of which was accommodated by West Walanae Fault and East Walanae Fault. For the southernmost region of the Arm region, there is the largest dilatation pattern reaching 0.7 μs which is accommodated by Lompobattang Volcano mixed with interpolation effects due to limited data in the south. The dilatation pattern is seen to divide the Walanae Fault System into two parts, namely the northern part which has an intermediate rate and southern dilatation pattern which has a larger dilatation pattern.

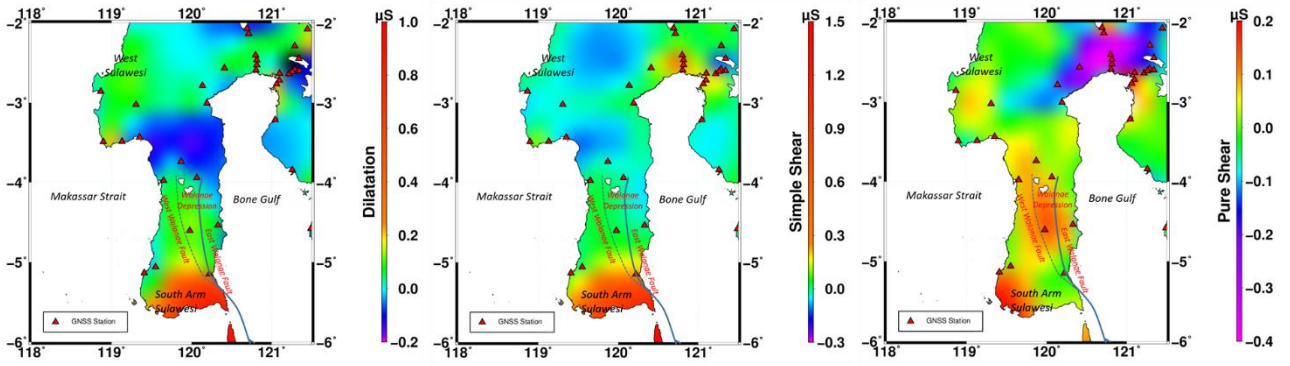

Fig. 4. Dilatation (left), simple shear (center) and pure shear (left) of South Sulawesi Arm

For the southernmost part of South Sulawesi Arm, the dominance of the high simple shear pattern (Figure 4 center) ranges from 0.3-1.3 μs and is divided into two parts pure shear pattern (Figure 4 right) which is between 0.1-0.2 μs in the Makassar region and -0.1-0.0 μs in the Bulukumba area with Lompobattang Volcano as the boundary. To the north of this region, changes in simple shear patterns can be seen that are almost homogeneous towards a minimum of 0.0 μs in the plutonic mountainous region. The change of pattern is seen to occur again separating the Walanae Fault System to the south with a high rate of simple shear and the northern part with a smaller simple shear. For the northern East Walanae Fault there is a change in the pattern in the northern part of Watampone, which is in the Sengkang East Basin that shrinks to the east, and in the northernmost part of the boundary this simple shear pattern is known to have Masupu Fault. This region's pure shear pattern shows a more varied pattern than simple shear. For northern Makassar, the pure shear pattern changes slightly up to 0.05 μs in Western Divide Mountain and decreases to 0.0 μs in the Bantimala area and then increases again in the area around Pare-pare. This increasing rate of pure shear did not take place because it subsequently decreased in the Plutonic Arc Mountains at northern part. As for the northern region of Bulukumba, the change in pattern has increased in the area of Walanae depression to 0.15 μs but has decreased in the easternmost region around Watampone. The value of pure shear in the Walanae Depression region has decreased again after collide with the Plutonic Arc Mountains. The change of pattern in pure shear is seen to separate the Walanae Fault System to the south with a small pure shear and the northern part with a larger pure shear, and a small pure shear pattern cutting in the east-west direction, where this indicates a widening process in Walanae Depression which is in line with the formation of the West Sengkang Basin in the eastern part of the South Arm.

Fault	slip rate		slip deficit	
	E (mm/yr)	N (mm/yr)	E (mm/yr)	N (mm/yr)
east walane fault				
northern part	-7.030	-0.974	-17.250	12.894
southern part	-6.623	-0.368	-17.552	12.278
west walanae fault				
northern part	4.003	2.116	-28.363	9.709
southern part	2.263	2.360	-26.338	9.420

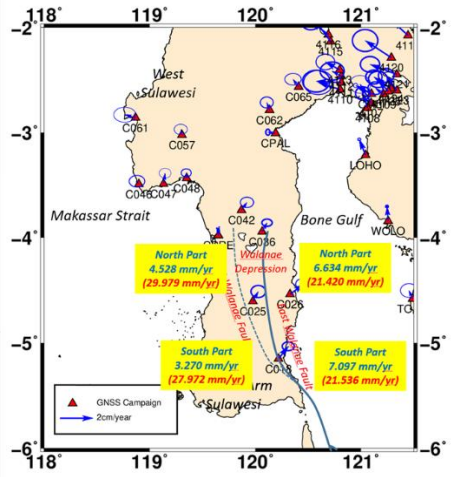

Fig. 5. Slip rate and slip deficit

Based on the dilation pattern, simple shear and pure shear described above, it can be seen that the Walanae Fault System can be divided into several strands, namely the northern and southern regions. By using a simple geometric modeling that is comparing the velocity rate of the station located in a different zone bounded by fault, we can estimate the slip rate of the fault and calculating the slip deficit based on the deficiency of the supposed rigid velocity of the Sunda Block on the station. Figure 5 shows the slip rate and slip deficit from the Walanae Fault System. The northern East Walanae Fault has an absolute slip rate of 6.634 mm / year with a slip deficit of 21.420 mm / year, and the southern part has a 7.097 mm / year of absolute slip rate with slip deficit of 21.536 mm / year. The northern part of West Walanae Fault has an absolute slip rate of 4.528 mm / year with a slip deficit of 29.979 mm / year and the southern part with an absolute slip rate of 3.270 mm / year and a deficit slip of 27,929 mm / year. The northern part of Walanae fault system has opening or spreading pattern occurs that is in harmony with the formation of Walanae depression and West Sengkang Basin at eastern part. By using simple geometric modeling, we found the fault system have 2 strain partitions with dominant sinistral strike slip pattern at southern part of Walanae Fault System (for both East and West Fault) and combination between sinistral / left lateral strike slip with thrust fault pattern at northen part of Walanae Fault System especially at East Walanae Fault. This is in line with the vertical movement of the fault system which indicates a graben pattern in the form of a surface drop in Walanae depression and a thrust fault positive (increasing) rate for the boundary area that limits this graben which is eastern part of the East Walanae Fault and in the western part of West Walanae Fault.

4 Conclusion

Walanae fault system did not only have one strand but was divided into 4 parts, namely the northern East Walanae Fault with a slip rate of 6.634 mm/year and the southern part with a 7.097 mm/year of slip rate, as well as the northern part of West Walanae Fault with a slip rate of 4.528 mm/year and the southern part with a slip rate of 3.270 mm/year. The northern part of Walanae fault system has opening or spreading pattern occurs that is in harmony with the formation of Walanae depression. By using simple geometric modeling, we found the fault system have 2 strain partitions with dominant sinistral strike slip pattern at southern part and combination between left lateral strike slip with thrust fault pattern at northern part. This is in line with the vertical movement of the fault system which indicates a graben pattern in the form of a surface drop in Walanae depression and a thrust fault positive (increasing) rate for the boundary area that limits this graben which is eastern part of the East Walanae Fault and in the western part of West Walanae Fault.

Deep appreciation and many thanks to Indonesian Geospatial Information Agency (BIG) and ITB for research collaboration. And deepest gratitude for Prof. C. Vigny, Dr. W.J.F. Simons, Prof. B. Sapiie and Prof. H.Z. Abidin, who provided knowledge to the author in the "state of the art" of geodynamic study using geodetic - technology and methods.

References

1. Hamilton, W. Tectonics of the Indonesian Region. U.S. Geological Survey Professional Paper 1078. (1979)
2. Yuwono, Y.S., Maury, R., Soeria-Atmadja, R., Bellon, H. Tertiary and Quaternary geodynamic evolution of South Sulawesi constraints from the study of volcanic units. Geologi Indonesia Jakarta 13, 32-48. (1988)
3. Coffield, D.Q., Bergman, S.C., Carrard, R.A., Guritno, N., Robinson, N.M., Talbot, J. Tectonic and stratigraphic evolution of the Kalosi PCS area and associated development of a Tertiary petroleum system, South Sulawesi, Indonesia. Proceedings of the Indonesian Petroleum Association 22 (1), 679-706. (1993)
4. Priadi, B., Polvé, M., Maury, R.G., Bellon, H., Soeria-Atmadja, R., Joron, J.L., Cotton, J. Tertiary and Quaternary magmatism in Central

Sulawesi: chronological and petrological constraints. Journal of Southeast Asian Earth Sciences 9 (1-2), 81-93. (1994)
5. Bergman, S.C., Coffield, D.Q., Talbot, J.P., Garrard, R.J. Tertiary tectonic and magmatic evolution of western Sulawesi and the Makassar Strait, Indonesia. Evidence for a Miocene continentecontinent collision. In: Hall, R., Blundell, D.J. (Eds.), Tectonic Evolution of SE Asia, Geological Society of London, Special Publications, vol. 106, pp. 391-430. (1996)
6. Polvé, M., Maury, R.C., Bellon, H., Rangin, C., Priadi, B., Yuwono, S., Joron, J.L., Soeria-Atmadja, R., Magmatic evolution of Sulawesi: constraints on the Cenozoic geodynamic history of the Sundaland active margin. Tectonophysics 272, 69-92. (1997)
7. Hall, R., Wilson, M.E.J.Neogene sutures in eastern Indonesia. Journal of Asian Earth Sciences 18, 781e808. (2000)
8. Hall, R.,. Cenozoic geological and plate tectonic evolution of SE Asia and the SW Pacific: computer-based reconstructions, model and animations. Journal of Asian Earth Sciences 20, 235-431. (2002))
9. Elburg, M., Foden, J.,. Geochemical response to varying tectonic settings: an example from Southern Sulawesi (Indonesia). Geochimica et Cosmochimica Acta 63, 1155-1172. (1999)
10. Jaya, A., and Nishikawa, O. Paleostress reconstruction from calcite twin and fault-slip data using the multiple inverse method in the East Walanae fault zone: implications for the Neogene contraction in South Sulawesi, Indonesia. Journal of Structural Geology, 34-49. (2013)
11. Van Bemmelen, R.W. The Geology of Indonesia, vol. 1a. Government Printing Office, The Hague, p. 732. (1949)
12. Van Leeuwen, T.M. The geology of southwest Sulawesi with special reference to the Biru area. In: Barber, A., Wiryosujono, S. (Eds.), The Geology and Tectonics of Eastern Indonesia. Geological Research and Development Centre, pp. 277-304. Special Publication 2. (1981)
13. Van Leeuwen, T.M., Susanto, E.S., Maryanto, S., Hadiwisastra, S., Sudijono, Muharjo. Tectonostratigraphic evolution of Cenozoic marginal basin and continental margin successions in the Bone Mountains, South Sulawesi, Indonesia.Journal of Asian Earth Sciences 38, 233-254. (2010)
14. Sukamto, R., Supriatna, S. The Geology of the Ujung Pandang, Benteng and Sinjai, Sulawesi. Geological Research and Development Centre, Bandung. Quadrangles Series, Scale 1: 250.000. (1982)
15. Sarsito, D.A. Pemodelan geometrik dan kinematik kawasan Sulawesi-Kalimantan Bagian Timur berdasarkan data GNSS-GPS dan Gayaberat Global , Disertasi, Institut Teknologi Bandung, Indonesia (2010)
16. Calvert, S.J., Hall, R. The Cenozoic geology of the Lariang and Karama regions, Western Sulawesi: new insight into the evolution of the Makassar Straits region. Proceedings of the Indonesian Petroleum Association 29, 501-557 (2003)
17. Berry, R.F., Grady, A.E. Mesoscopic structures produced by Plio-Pleistocene wrench faulting in South Sulawesi, Indonesia. Journal of Structural Geology 9, 563-571. (1987)
18. Nikolaidis, R. M. *Observation of geodetic and seismic deformation with the Global Positioning System*, Disertasi, University of California, San Diego (2002)